International Food Research Journal 30(4): 924 - 932 (August 2023)
Journal homepage: *http://www.ifrj.upm.edu.my*

Histamine-regulated brain-derived neurotrophic factor (BDNF) catabolism by specific gut microbiota in mice

[1]Luo, Q.-Q., [1]Shi, R.-Y., [1]Liu, Y.-T., [2]Huang, L.-B., [1]*Chen, W. and [1]Wang, C.-T.

[1]Beijing Advanced Innovation Center for Food Nutrition and Human Health, Beijing Engineering and Technology Research Center of Food Additives, School of Food and Health, Beijing Technology and Business University, Beijing 100048, P. R. China
[2]College of Animal Science and Technology, Shandong Agricultural University, Taian 271000, P. R. China

Article history

Received:
6 October 2022
Received in revised form:
6 December 2022
Accepted:
10 February 2023

Keywords

Huangjiu,
histamine,
gut microbiota,
gut-brain axis,
brain-derived neurotrophic factor

Abstract

Huangjiu usually causes excessive intoxication. Although the primary components, including β-benzyl ethanol, isopentanol, histamine, and phenethylamine are linked to intoxication, the underlying mechanism remains obscure. The present work thus analysed the effects of oral treatment of these components, particularly histamine, and discovered which of these components induced oxidative stress and inflammatory cytokine responses in mice serum and cerebrum. Lipopolysaccharide levels were elevated, and the gut microbiota was recomposed. Additionally, the catabolic pathway of the brain-derived neurotrophic factor was investigated. The correlation analysis revealed a possible correlation between gut microbiota changes and neurotransmitter imbalance. Based on the findings, histamine might alter the gut microbiota composition, affect the inflammatory LPS accumulation, and modulate the gut-brain axis, thus leading to an increase in oxidative stress, inflammatory response, and neurotransmitter imbalance in the brain. The present work provided a baseline for future research into the effects of Huangjiu, and enhanced our understanding of treating and preventing associated inflammatory diseases.

DOI
https://doi.org/10.47836/ifrj.30.4.10

Introduction

Huangjiu (Chinese rice wine) has a 7,000-year history (Li *et al*., 2020). The primary components of Huangjiu include carbohydrates, amino acids, organic acids, and lipids (Wu *et al*., 2015). However, Huangjiu does include several compounds that negatively affect its taste, flavour, and safety (Liu *et al*., 2016), resulting in unfavourable taste and excessive intoxication. β-benzyl ethanol (β-be) and isopentanol (Iso) were found to have the greatest impact on Huangjiu-induced excessive intoxication, followed by histamine (His) and phenylethylamine (PEA). These compounds caused varying levels of physiological imbalance in *Cyprinus carpio* (common carp). However, the underlying mechanism has not been explored (Sun *et al*., 2020).

The microbiota-gut-brain axis (MGB) is a neuroendocrine system that connects the gut microbiota and brain to regulate normal physiological functions (Goyal *et al*., 2021). Gut-brain communication relies on serotonin (5-HT) (Xie *et al*., 2020). The communication path is bidirectional, and gut microbiota may also control the gut-brain axis functions (Sandhu *et al*., 2017). The composition of the gut microbiota and the metabolites cause imbalances of neurotransmitters, *e.g*., lipopolysaccharides (LPS) (Winek *et al*., 2016). Additionally, the gut microbiota has been found to be involved in the inflammatory and immune responses, central and peripheral (intestinal) neurotransmissions, and glucose metabolism (Liu *et al*., 2019). Consequently, neurotransmitter imbalances and inflammation may be influenced by gut microbial composition and related metabolites, resulting in various physiological disorders, and a decline in cognitive and behavioural abilities (De-Ture and Dickson, 2019).

The present work thus aimed to investigate whether the four primary components of Huangjiu cause brain damage (measured by neuroinflammation and neurotransmitter imbalance) *via* regulating the

*Corresponding author.
Email: weichen@btbu.edu.cn

gut-brain axis. With oral treatment, oxidative stress and inflammatory cytokines increased significantly in the serum and cerebrum. Microbial structure and metabolism in the gut were altered. Moreover, the catabolic pathway of brain-derived neurotrophic factor (BDNF) in the brain was evaluated. The four components, especially His, appeared to cause brain damage in mice by regulating the gut-brain axis. Oral His treatment resulted in significant changes in the gut microbiota, resulting in increased levels of LPS, which further caused inflammation and oxidative stress in the brain, leading to neuroinflammation and neurotransmitter imbalance.

Materials and methods

Materials

The ELISA kits for brain-derived neurotrophic factor (BDNF), CREB, ERK1/2, and lipopolysaccharides (LPS) were purchased from Jiangsu Meimian Industrial Co., Ltd. (Yancheng, China). All additional chemical reagents and assay kits were of analytical quality, and used according to Luo *et al.* (2022).

Animals

A total of 36 healthy male C57BL/6J SPF mice [SCXK(Jing)2016-0006] were obtained from Beijing Vital River Laboratory Animal Center, acclimated for one week in advance, fed with a normal pellet chow diet (corn and soybean meal) and clean drinking water. The experimental conditions were strictly applied in the acclimatisation process, including temperature control at 22 ± 2°C, 65 ± 5% relative humidity, and a 12-h light/dark cycle. All the experimental procedures in the present work involving animals were approved by the Beijing Key Laboratory of Functional Food from Plant Resources (approval number: A103-2021). All mice were randomly assigned to six different groups (n = 6), namely Normal, β-be, Eth, His, PEA, and Iso groups for subsequent analyses.

Preparation and intervention of reagents with animals

The control and the Normal group both received saline by gavage at the same frequency. The Eth group received 15% (v/v) ethanolic solution; while the His, PEA, β-be, and Iso group received ethanolic solution (15%, v/v) of His, PEA, β-be, and Iso, respectively, by gavage once daily, for two weeks. The gavage dose for all the above operations was 15 mL/kg BW. The experimental design was according to Luo *et al.* (2022) (Figure 1). Peng *et al.* (2019) determined the specific doses of these substances, and the specific doses for gavage are presented in Table 1.

In the present work, the concentration of the four substances was determined using the absorption of each substance per kilogram of body weight in adults. The dose was established in mice based on the consumption of two 500 mL bottles of Huangjiu by adults weighing 60 kg. All experimental groups received normal food and water.

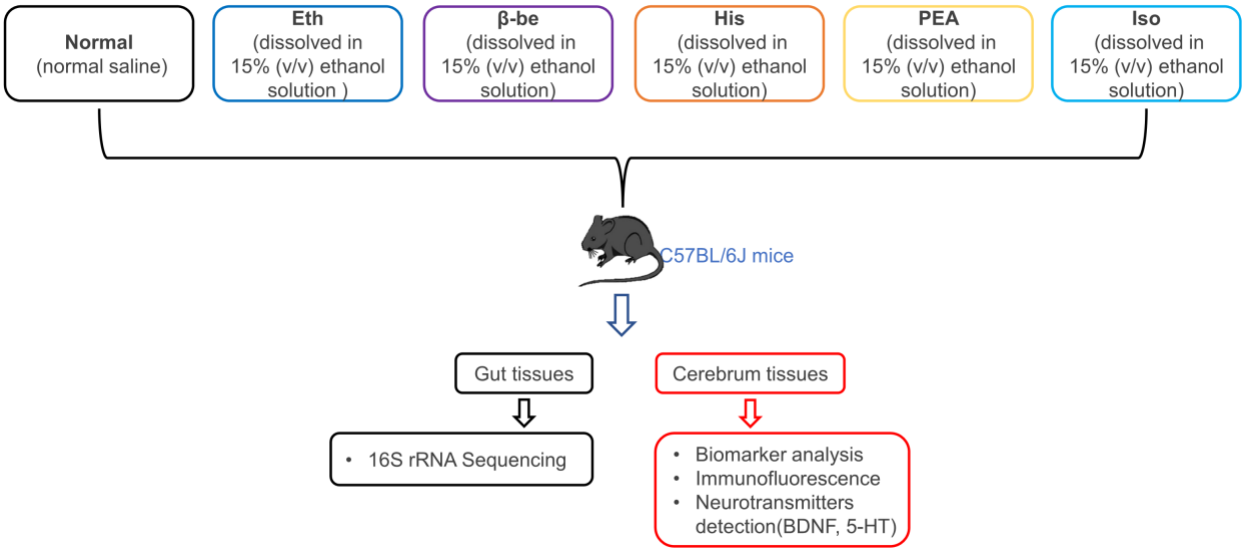

Figure 1. Experimental design.

Table 1. Dosage of each compound in mice.

Compound	Content in Huangjiu (mg/L)	Dosage in mice (mg/25g.bw)
His	17.00	0.14
PEA	117.97	0.98
Iso	189.26	1.58
β-be	128.61	1.07

Mice stool was collected in sterile sampling tubes at the end of the experiment, and frozen for subsequent use. After all the experiments, 12-h fasting mice were sacrificed by CO_2 asphyxiation in a covered container attached to a CO_2 tank. The serum was then collected and centrifuged at 3,000 rpm for 10 min at 4°C before being stored at -80°C.

The cerebrum and gut tissues were washed with pre-cooled normal saline, and adhesive serum was removed. Tissues were weighed and cut into pieces. These pieces were then partly immersed in 4% DPEC (dissolved in PBS, v/v) and partly added to nine times 0.9% saline. Tissues were ground to prepare a 10% (w/v) homogenate in an ice bath, centrifuged at 12,000 rpm for 15 min at 4°C. The supernatant was then removed and stored at -80°C for future use.

Biomarker analysis of serum and cerebrum tissues

Malondialdehyde (MDA), reduced glutathione (GSH), interleukin (IL)-6, interleukin (IL)-10, superoxide dismutase (SOD), and tumour necrosis factor (TNF)-α were the biomarkers that were analysed *via* kits in serum and cerebrum tissues. All experimental procedures were performed following the manufacturer's instructions.

Histopathological analysis of cerebrum tissues

Cerebrum tissue prepared in 4% DPEC was further dehydrated, embedded in paraffin, and stained with haematoxylin and eosin. The slices were then examined under the panoramic microscope in the lab (3D HITECH Panimal 250, Hungary).

Validation of BDNF pathway

The BDNF, CREB, and ERK1/2 levels of the cerebrum were analysed using ELISA kits to perform validation of the BDNF pathways. All experimental procedures were performed following the manufacturer's instructions.

Determination of LPS in gut tissues, and 5-HT in cerebrum tissues

The LPS level in the gut tissues and the 5-HT levels in the cerebrum tissues were measured using ELISA kits. All experimental procedures were performed following the manufacturer's instructions.

Analysis of gut microbiota diversity

16S rRNA analysis was performed using pre-frozen stools to determine the composition and structure of the gut microbial community. DNA of stool sample was extracted and sequenced. The V3 - V4 hypervariable region was amplified using universal plots 338F and 806R (Wang *et al*., 2007). Illumina MiSeq PE300/NovaSeq PE250 platforms (Illumina, San Diego, USA) were used to sequence purified amplicons in equimolar pools with paired-end sequencing as per Major Bio Bio-Pharm Technology Co. Ltd. (Shanghai, China)'s standard protocols. With a 97% similarity cut-off, operational taxonomic units (OTUs) were clustered using UPARSE 7.1 (Stackebrandt and Goebel, 1994; Edgar, 2013). The chimeric sequences were identified and removed. Each OTU representative sequence's taxonomy was analysed using RDP Classifier version 2.2 (Wang *et al*., 2007), based on a confidence threshold of 0.70 against the 16S rRNA database.

Correlation analysis between gut microbiota and neurotransmitters

Spearman correlation analysis was used to explore the potential mechanisms for the association between gut microbiota and LPS, as well as LPS and neurotransmitters. The correlation was considered significant when the absolute correlation coefficient was greater than 0.6 (p-value < 0.05).

Statistical analysis

Results were expressed as means ± SD. When $p < 0.05$, the result was considered significant, and the

data were evaluated using One-way ANOVA. GraphPad Prism version 8.0 (California, USA) was used to analyse all data.

Results

Four components affected body weight, cerebrum weight, and oxidative stress in mice

His group had a significantly higher cerebrum weight ($p < 0.01$; Figure 2A) than the other five groups. In the cerebrum-to-body weight ratio, there was a similar tendency ($p < 0.01$; Figure 2B). The results of the cerebrum weight, serum, and cerebrum markers are depicted in Figures 2C and 2D. The serum GSH and SOD were significantly higher in the His and Iso groups than in the other groups ($p < 0.01$; Figure 2C). The serum MDA in the Normal group was significantly lower ($p < 0.01$; Figure 2C), while the Normal group had significantly higher cerebrum GSH than the other groups ($p < 0.01$; Figure 2D). Significant differences ($p < 0.01$) were seen in the cerebrum SOD and MDA amongst the six groups (Figure 2D).

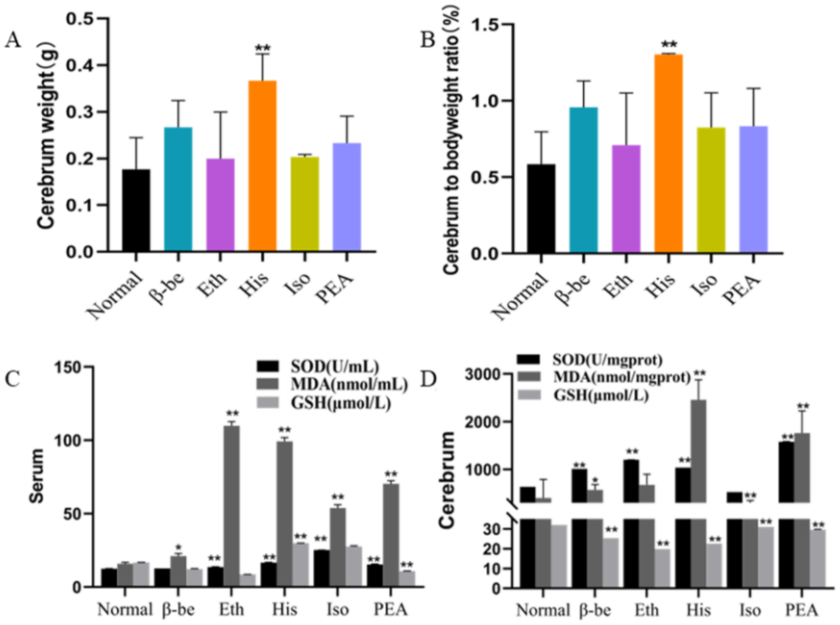

Figure 2. Effects of His, PEA, β-be, and Iso on cerebrum weight, serum, and levels of oxidative stress of mice in cerebrum and serum. *$p < 0.05$, **$p < 0.01$, $^{\#}p < 0.05$ compared with Normal. **(A)** Cerebrum weight, **(B)** cerebrum to bodyweight ratio, **(C)** levels of oxidative stress in serum, and **(D)** levels of oxidative stress in cerebrum.

Four components affected inflammatory cytokines in cerebrum and serum of mice

The representative histological cerebrum results using H&E revealed two inflammatory lesions on the cerebrum surface (as marked by the arrows). The His group (Figure 3C) had an increased number of gaps between the neurons near the lesions and surrounding tissues compared to the Normal (Figure 3A), Eth (Figure 3B), and other groups (Figure 4). As shown in Figures 3D and 3E, the levels of TNF-α and inflammatory cytokines in His group, both in the cerebrum and serum, showed a significant increase compared to the other groups. The serum IL-10 levels in the β-be, His, and Iso groups were significantly lower than the Normal group (Figures 3D and 3E).

Four components affected BDNF pathway, 5-HT, and LPS in mice

BDNF in the His group had significantly lower levels compared to other groups ($p < 0.01$) (Figure 5A). Additionally, His had significantly higher levels of CREB ($p < 0.01$) compared to other groups (Figure 5B). Furthermore, the β-be group had a significantly lower BDNF level than the Normal group, while the His group had a significantly lower ERK1/2 level than the Normal and β-be group, respectively ($p < 0.01$; Figure 5C). The His group exhibited significantly higher levels of gut LPS and cerebrum 5-HT than in other groups (Figures 5D and 5E; $p < 0.01$).

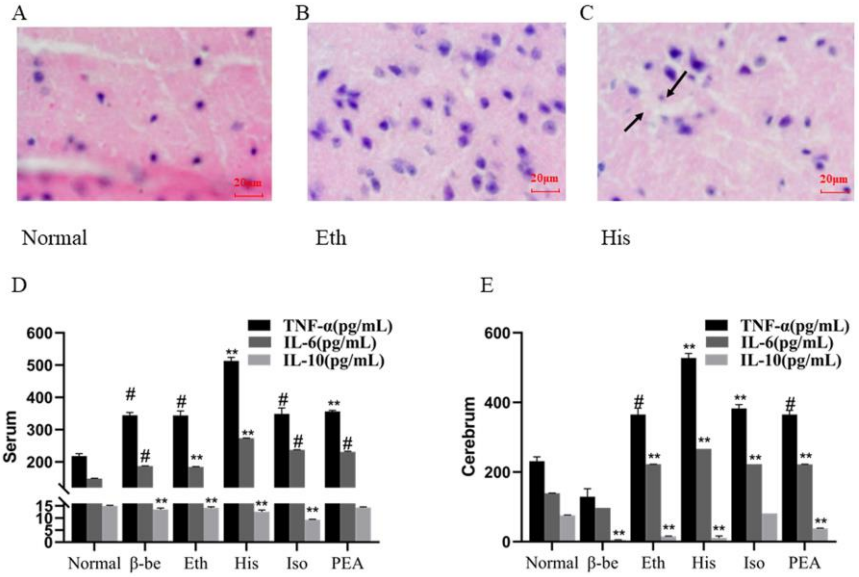

Figure 3. Effects of His, PEA, β-be, and Iso on the levels of oxidative stress of mice in the cerebrum and serum, and representative histological cerebrum results using H&E. $*p < 0.05$, $**p < 0.01$, $^{\#}p < 0.05$ compared with Normal. **(A)** Representative histological cerebrum results using H&E in Normal, **(B)** representative cerebrum histological results using H&E in Eth, **(C)** representative histological cerebrum results using H&E in His, **(D)** level of inflammatory cytokines in serum, and **(E)** level of inflammatory cytokines in cerebrum.

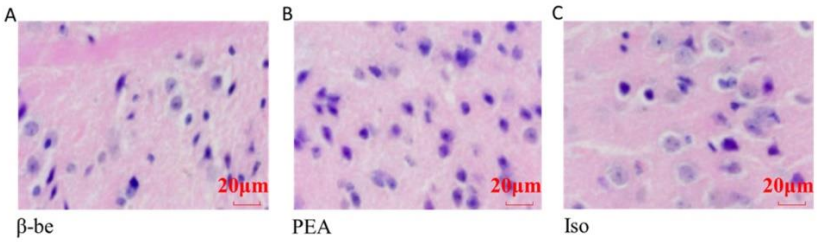

Figure 4. Representative histological cerebrum results using H&E in PEA, β-be, and Iso.

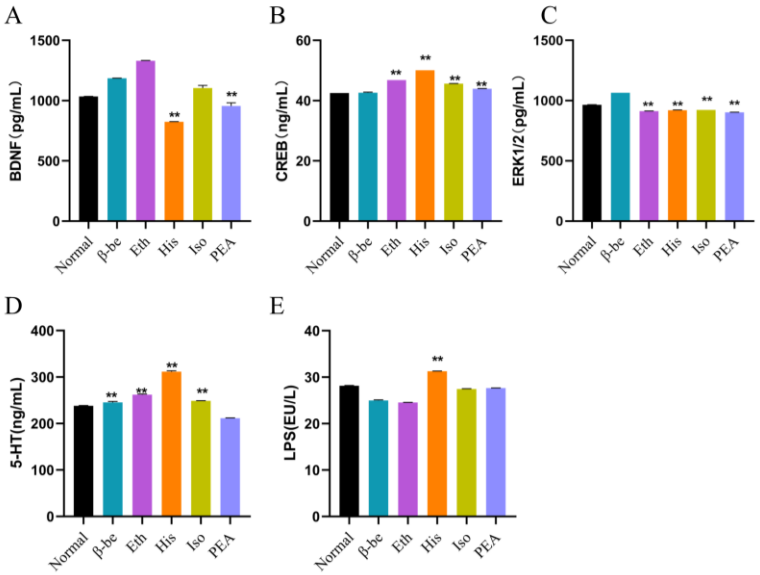

Figure 5. Effects of His, PEA, β-be, and Iso on the BDNF pathway and 5-HT in cerebrum and gut LPS. $**p < 0.01$. **(A)** Cerebrum BDNF, **(B)** cerebrum CREB, **(C)** cerebrum ERK1/2, **(D)** cerebrum 5-HT, and **(E)** gut LPS.

Four components affected the gut microbial community structure and composition of mice

A total of 780,661 raw readings were obtained from the six groups of 18 faecal samples mentioned earlier (n = 6), and the average reads of each sample were 43,370. There were significant differences in Ace, Shannon, and Simpson indexes among different groups (Figure 6). The His group had significantly lower Ace, Shannon, and Simpson indices than the Normal group (Figures 6A, 6B, and 6C). Furthermore, the β-be group had a significantly lower Ace index than the Normal group (Figure 6A). Normal group had a higher Simpson index than all other groups (Figure 6B). Eth group exhibited a lower Shannon index than the Normal group (Figure 6C). Additionally, there was no significant difference in Chao index across all six groups (Figure 6D). The relationship among all six treatments and the gut microbiota was validated using principal coordinate analysis and coordinate plots (Figure 6E). The results of the Circos analysis at the phyla level validated the differences in gut microbial diversity among the six different groups (Figure 6F). Proteobacteria and Cyanobacteria were unique to the Normal group. The His group had the lowest relative abundance of Firmicutes.

A total of 613 operational taxonomic units (OTUs) were detected in all faecal samples, including 19 phyla and 213 genera. Different treatments resulted in differences in the structural composition of microbial communities at the phylum and genus levels in the gut. The dominant phyla were Bacteroides, Firmicutes, Proteobacteria, Cyanobacteria, and Deferribacterota (Figure 6G). *norank_f__Muribaculaceae*, *Prevotellaceae_UCG-001*, *Lachnospiraceae_NK4A136_group*, *unclassified_f__Lachnospiraceae*, and *Alistipes* were the predominant genera (Figure 6H).

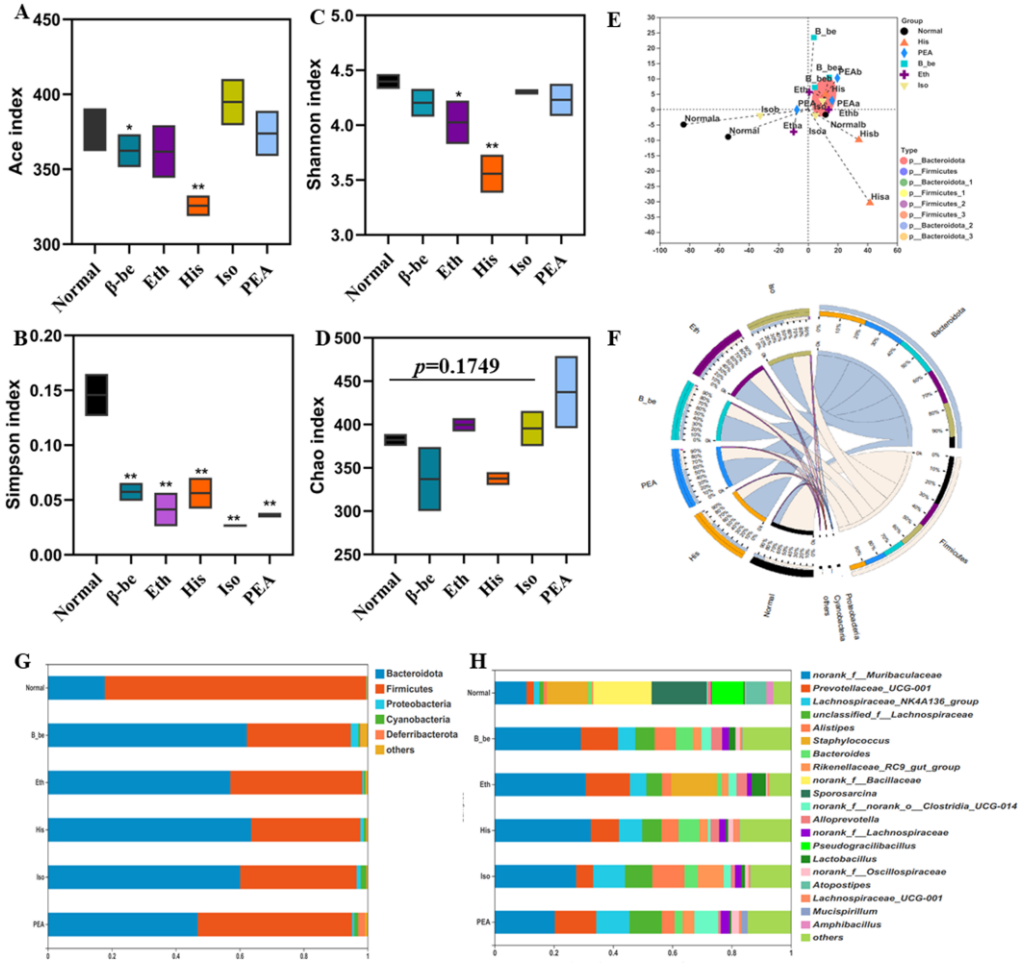

Figure 6. Effects of His, PEA, β-be, and Iso on gut microbiome in mice. *p < 0.05, **p < 0.01. **(A)** Ace index, **(B)** Simpson index, **(C)** Shannon index, **(D)** Chao index, **(E)** Principal coordinate analysis, **(F)** Circos analysis, **(G)** relative abundance plot at phylum level of gut microbiota, and **(H)** relative abundance plot at genus level of gut microbiota.

Correlation between gut microbiota and biomarkers

Spearman correlation analysis was performed on the levels of the neurotransmitter, gut microbiota, and microbial metabolites in mice among the six different treatment groups (Figure 7). Results showed a negative correlation ($p < 0.05$) between the relative abundance of *Lactobacillus* and the LPS levels in the gut. Moreover, the relative abundance of *Prevotellaceae_UCG-001* and the ERK1/2 levels were negatively correlated ($p < 0.05$), the relative abundance of *norank_f__Muribaculaceae* and the levels of CREB and 5-HT were positively correlated ($p < 0.05$), and the relative abundance of *Alloprevotella* and the 5-HT level were positively correlated ($p < 0.05$). Furthermore, the relative abundance of *Ruminococcus* and the BDNF were negatively correlated, whereas the CREB level was positively correlated ($p < 0.05$).

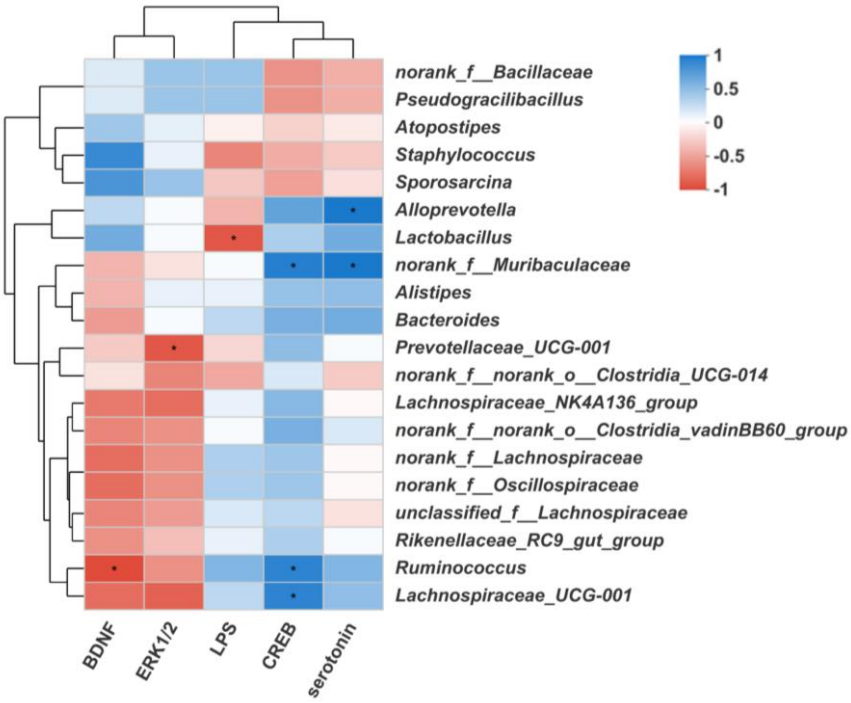

Figure 7. Spearman's correlation among gut microbiome, LPS, and the levels of 5-HT, BDNF, CREB, and ERK1/2 of mice. *$p < 0.05$.

Discussion

High dietary biogenic amine intake may cause physical discomforts such as skin redness, headache, nausea, palpitation, and unstable blood pressure (Linares *et al*., 2016). As discovered by Sun *et al*. (2020), β-be, Iso, His, and PEA had the greatest impact on Huangjiu-induced excessive intoxication. Therefore, the four components were selected for analysis.

Gut microbiota is associated with normal neurodevelopmental disorders (Winek *et al*., 2016; Sampson *et al*., 2016). Results from 16 observational and 11 clinical studies showed gut microbiota changes in 424 patients with severe depression and gut barrier cutting (Jing *et al*., 2021). The increase in pro-inflammatory cytokines is among the crucial manifestations of some nervous system diseases (Wei *et al*., 2019). In the present work, the TNF-α and IL-6 levels in the His group significantly increased than in any other group ($p < 0.01$), indicating that the His treatment may result in neuroinflammation.

The intestinal epithelium can receive signals in the form of microbial metabolites (such as LPS, short-chain fatty acids, *etc*.) from the gut microbiota, thus maintaining normal physiological functions of the intestinal mucosal barrier (Nadjsombati *et al*., 2018). LPS primarily activated NFκB, causing excessive inflammatory responses. Inflammatory responses were reflected by elevated levels of cytokines (IL-6 and TNF-α) (Zhan *et al*., 2018). In the present work, His treatment significantly increased the gut LPS levels. Furthermore, the cerebrum IL-6 and TNF-α levels in the His group increased significantly ($p < 0.01$), thus resulting in brain inflammation.

In the present work, His treatment significantly increased the 5-HT level ($p < 0.01$), indicating that His treatment might cause neuroinflammation and an imbalance in the gut microbiome through the increase in the 5-HT level. Neurotrophic factors, such as BDNF, were observed to promote the growth, development, differentiation, maturation, and survival of neurons in the nervous system (Siresha and Das, 2015; Di *et al*., 2019). After binding with Tr*κ*B, BDNF activated downstream serine/threonine kinases, and then MAPK/ERK kinases and ERK, ultimately leading to phosphorylation of CREB (Siresha and Das, 2015). In the present work, the His group decreased BDNF and ERK1/2 levels, suggesting that His treatment might cause the neurotransmitter imbalance.

To further explore the underlying mechanism, the community succession of the gut microbiome was detected after various treatments *via* 16S rRNA sequencing. The findings revealed that His treatment increased the relative abundance of Proteobacteria, indicating the occurrence of dysbiosis (Li *et al*., 2017). At the genus level, His treatment promoted *Lachnospirace-ae_NK4A136_group* and *norank_f_Lachnospiracae* relative abundance, which was reported to be increased by Fubrick tea attenuates (Shin *et al*., 2015). The His group exhibited a lower relative abundance of *Lactobacillus* than other groups. The His group increased *Ruminococcus* relative abundance but decreased *Lactobacillus* relative abundance, indicating that His may increase intestinal stress and cause the gut microbiome imbalance.

Conclusion

To summarise, four primary components of Huangjiu increased metabolic disturbances, oxidative stress, and neurotransmitter imbalances and body inflammation in mice by modulating the gut microbiome and metabolites. In particular, His treatment altered the gut microbiome composition (for example, *Ruminococcus* and *Lactobacillus*), increasing inflammatory LPS and oxidative stress, thus resulting in inflammatory damage and neurotransmitter imbalance. Further exploration is required to understand the comprehensive relationship between the gut microbiome and neurotransmitter metabolism.

Acknowledgement

The present work was financially supported by Beijing Municipal Natural Science Foundation, Beijing Municipal Education Commission on Science and Technology Plan Key Joint Project (grant no.: KZ202010011016); Beijing Engineering Technology Research Center Platform Construction Project (grant no.: 19008021109); Construction of High-Precision Disciplines in Beijing-Food Science and Engineering [(grant .: no,19008021085), and Cultivation Project of Double First-Class Disciplines of Food Science and Engineering, Beijing Technology and Business University (grant no.: BTBUYXTD202208).

References

De-Ture, M. and Dickson, D. 2019. The neuropathological diagnosis of Alzheimer's disease. Molecular Neurodegeneration 14: 32-39.

Di, C., Punzi, G. and Ursini, G. 2019. Brain-derived neurotrophic factor and schizophrenia. Psychiatric Genetics 29: 200-210.

Edgar, R. 2013. UPARSE: Highly accurate OTU sequences from microbial amplicon reads. Nature Methods 10: 996-998.

Goyal, D., Ali, S. A. and Singh, R. K. 2021. Emerging role of gut microbiota in modulation of neuroinflammation and neurodegeneration with emphasis on Alzheimer's disease. Progress in Neuro-Psychopharmacology and Biological Psychiatry 106: 110-112.

Jing, N., Liu, X., Jin, M., Yang, X., Hu, X. and Li, C. 2021. Fubrick tea attenuates high-fat diet-induced fat deposition and metabolic disorder by regulating gut microbiota and caffeine metabolism. Food and Function 11: 6971-6980.

Li, W., Fan, G., Fu, Z., Wang, W., Xu, Y., Teng, C., … and Li, X. 2020. Effects of fortification of *Daqu* with various yeasts on microbial community structure and flavor metabolism. Food Research International 129: 108837.

Li, Y., Xia, B., Li, R., Yin, D., Wang, Y. and Liang, W. 2017. Expression of brain-derived neurotrophic factors, neurotrophin-3, and neurotrophin-4 in the nucleus accumbens during heroin dependency and withdrawal. Neuroreport 28: 654-660.

Linares, D., del Rio, B., Redruello, B., Ladero, V. and Martin, M. 2016. Comparative analysis of the *in vitro* cytotoxicity of the dietary biogenic amines: Tyramine and histamine. Food Chemistry 197: 658-663.

Liu, P., Wu, L., Peng, G., Han, Y., Tang, R. and Ge, J. 2019. Altered microbiomes distinguish Alzheimer's disease from amnestic mild cognitive impairment and health in a Chinese cohort. Brain, Behavior, and Immunity 80: 633-643.

Liu, S., Yu, J., Wei, X., Ji, Z., Zhou, Z. Meng, X. and Mao, J. 2016. Sequencing-based screening of functional microorganisms to decrease the formation of biogenic amines in Chinese rice wine. Food Control 64: 98-104.

Luo, Q., Shi, R., Liu, Y., Huang, L., Chen, W. and Wang, C. 2022. Histamine causes pyroptosis of liver by regulating gut-liver axis in mice. International Journal of Molecular Science 23: 3710-3725.

Nadjsombati, M., McGinty, J., Lyons-Cohen, M., Jaffe, J., DiPeso, L., Schneider, C. and Miller, N. 2018. Detection of succinate by intestinal tuft cells triggers a type 2 innate immune circuit. Immunity 49: 33-41.

Peng, L., Liu, S., Ji, Z., Chen, S. and Mao, J. 2019. Structure characterization of polysaccharide isolated from Huangjiu and its anti-inflammatory activity through MAPK signaling. International Journal of Food Science and Technology 54: 1874-1883.

Sampson, T. R., Debelius, J. W., Thron, T., Janssen, Shastri, G. G., … and Mazmanian, S. K. 2016. Gut microbiota regulate motor deficits and neuroinflammation in a model of Parkinson's disease. Cell 167: 1469-1480.e12.

Sandhu, K. V., Sherwin, E., Schellekens, H., Stanton, C., Dinan, T. and Cryan, J. 2017. Feeding the microbiota-gut-brain axis: Diet, microbiome, and neuropsychiatry, Translational Research: 179: 223-244.

Shin, N., Whon, T. and Bae, J. 2015. Proteobacteria: Microbial signature of dysbiosis in gut microbiota. Trends in Biotechnology 33: 496-503.

Siresha, B. and Das, U. 2015. Brain-derived neurotrophic factor and its clinical implications. Archives of Medical Science 11: 1164-1178.

Stackebrandt, E. and Goebel, B. 1994. Taxonomic note: A place for DNA-DNA reassociation and 16s rRNA sequence analysis in the present species definition in bacteriology. International Journal of Systematic Bacteriology 44: 846-849.

Sun, H., Liu, S., Mao, J., Yu, Z., Lin, Z. and Mao, J. 2020. New insights into the impacts of huangjiu components on intoxication. Food Chemistry 317: 126420.

Wang, Q., Garrity, G., Tiedje, J. and Cole, J. 2007. Naive Bayesian classifier for rapid assignment of rRNA sequences into the new bacterial taxonomy. Applied and Environmental Microbiology 73: 5261-5267.

Wei, L., Li, Y., Tang, W. and Sun, Q. 2019. Chronic unpredictable mild stress in rats induces colonic inflammation. Frontiers in Physiology 10: 1228-1239.

Winek, K., Dirnagl, U. and Meisel, A. 2016. The gut microbiome as a therapeutic target in central nervous system diseases: Implications for stroke. Neurotherapeutics 13: 762-774.

Wu, Z. Z., Xu, E. B. and Long, J. 2015. Measurement of fermentation parameters of Chinese rice wine using Raman spectroscopy combined with linear and non-linear regression methods. Food Control 56: 95-102.

Xie, Y., Chong, W., Di, Z., Chao, W. and Li, C. 2020. Dietary proteins regulate serotonin biosynthesis and catabolism by specific gut microbes. Journal of Agriculture Food Chemistry 68: 5880-5890.

Zhan, X., Stamova, B. and Sharp, F. 2018. Lipopolysaccharide associates with amyloid plaques, neurons and oligodendrocytes in Alzheimer's disease brain: A review. Frontiers in Aging Neuroscience 10: 42-59.